Normal SPECT Thallium-201 Bull's-eye Display: Gender Differences

Robert L. Eisner, Margery J. Tamas, Karen Cloninger, David Shonkoff, Joel A. Oates, Anita M. Gober, Daniel W. Dunn, John A. Malko, André L. Churchwell, and Randolph E. Patterson

The Carlyle Fraser Heart Center, Crawford Long Hospital of Emory University, Emory University School of Medicine, Department of Medicine/Division of Cardiology, Atlanta, Georgia; Emory University School of Medicine, Department of Radiology, Atlanta, Georgia; and Digital Design, Inc., Norcross, Georgia

The bull's-eye technique synthesizes three-dimensional information from single photon emission computed tomographic ^{201}Tl images into two dimensions so that a patient's data can be compared quantitatively against a normal file. To characterize the normal database and to clarify differences between males and females, clinical data and exercise electrocardiography were used to identify 50 males and 50 females with < 5% probability of coronary artery disease. Results show inhomogeneity of the ^{201}Tl distributions at stress and delay: septal to lateral wall count ratios are < 1.0 in both females and males; anterior to inferior wall count ratios are > 1.0 in males but are approximately equal to 1.0 in females. Washout rate is faster in females than males at the same peak exercise heart rate and systolic blood pressure, despite lower exercise time. These important differences suggest that quantitative analysis of single photon emission computed tomographic ^{201}Tl images requires gender-matched normal files.

J Nucl Med 29:1901–1909, 1988

A major advance in analysis of single photon emission computed tomographic (SPECT) thallium-201 (^{201}Tl) myocardial perfusion scans is the quantitation of stress, delay, and washout data (*1–4*). To carry out this analysis, it is necessary to define quantitatively the normal range of ^{201}Tl distribution within the heart. The purpose of the present study is to answer the following questions:

1. What is the variability in myocardial ^{201}Tl distribution among normal individuals?
2. Are there systematic differences in the ^{201}Tl distribution to different regions of the normal heart?
3. Does the myocardial ^{201}Tl distribution differ between females and males?
4. Does the ^{201}Tl washout rate between stress and 3-hr delay images vary among different regions of the normal heart?
5. Does it vary between females and males?

Received Apr. 6, 1988; revision accepted July 22, 1988.

For reprints contact: Randolph E. Patterson, MD, Carlyle Fraser Heart Center, Crawford Long Hospital of Emory University, 550 Peachtree Street, NE, Suite 4323, Atlanta, GA 30365.

* Preliminary data for this paper were presented at the 34th Annual Meeting of the Society of Nuclear Medicine, June 2–5, 1987, Toronto, Ontario, Canada.

Detailed answers to these questions are required to use effectively a normal reference file for the quantitative comparison of each new patient being tested against the expected range of normals. The data are analyzed and displayed using the bull's-eye format (*4*).

METHODS

Study Population

We studied 130 females and 180 males who were referred for exercise ECG and SPECT myocardial ^{201}Tl imaging by their attending physicians. When the patient came to the exercise laboratory after an overnight fast, she or he was interviewed by a cardiologist who characterized the presence or absence of the following risk factors for coronary artery disease (CAD): smoking, hypertension, diabetes, elevated cholesterol, and abnormal resting ECG. Next, each patient was interviewed concerning a history of chest discomfort. The discomfort was characterized according to the following three features: (1) location in the chest, whether central or lateral; (2) duration, whether it was 2–20 min, briefer, or more prolonged; and finally (3) whether it was induced by exercise and relieved by rest. The pain was characterized as "typical angina pectoris" if it showed all three features, i.e., was located in the center of the chest, lasted 2–20 min, and was precipitated by exercise and relieved by rest. If the pain showed only two of these three characteristics it was considered "atypical chest pain," and if the pain showed only one of the three characteristics, then it was called "nonanginal chest pain."

Exercise Testing

After this interview, the cardiologist supervised a symptom-limited exercise treadmill test according to the Bruce protocol while a 12-lead ECG was recorded as described previously (*5*). The resting ECG was analyzed for baseline ST-T wave abnormality, evidence of prior myocardial infarction (Q waves > 0.03 sec that were at least ¼ the depth of the R wave) and left ventricular hypertrophy. No patient selected for this study had prior myocardial infarction. The criterion for a positive ECG response to exercise was 0.1 mV flat or downsloping ST segment depression 0.08 sec after the J point in at least three consecutive heart beats with a normal baseline ST-T wave segment. If the baseline ECG was abnormal or if the patient was taking digitalis, then the test was called equivocal if there was at least 0.1 mV flat or downsloping ST segment depression. No patient selected for analysis of normal ^{201}Tl distribution was taking digitalis or had a positive exercise ECG. In addition, the patient was required to reach 85% of age-predicted maximum heart rate to be included in this analysis of normal ^{201}Tl distribution. The patients were exercised to a symptomatic end-point of chest discomfort, dyspnea, fatigue, or leg discomfort. Patients were not stopped simply because of achieving a target heart rate, but would have been stopped for cardiac arrhythmias or ST segment depression if it exceeded 0.2–0.3 mV. Patients had an i.v. catheter placed before the exercise test and were asked to tell the physician when they felt that they could only exercise for 60 sec more, at which time 3.5 mCi ^{201}Tl was injected.

Definition of "Normal" Subject

Without knowledge of ^{201}Tl results, we selected 73 females and 77 males from the 310 subjects analyzed as "normal" subjects based on their having < 5% probability of CAD, from a nomogram (*6*) that summarized Framingham Study data for age, sex and risk factors (*7*) and the summary of chest pain histories by Diamond and Forrester (*8*). Exercise ECG results (chest pain or ST depression) were included in the nomogram for sequential Bayesian analysis of clinical and test data (*6*). Briefly, no patient had more than three risk factors; no woman had typical angina although some had atypical chest pain; no man had atypical chest pain although some had nonanginal chest pain; and no woman or man had a positive exercise ECG-ST response or chest pain on the treadmill although some had equivocal tests. All subjects had to achieve at least 85% age-predicted maximum heart rate for this analysis. The final probability of CAD based on age, sex, risk factors, chest pain history, and exercise ECG results was < 5%. Most subjects had much less than 5% probability of CAD, but we included a few older subjects with negative screening tests to achieve broad age representation.

All subjects selected had been referred by their private physicians for clinical reasons, and none were volunteers. All patients were identified as normal (< 5% probability of CAD) without knowledge of their ^{201}Tl data. We identified 73 females and 77 males as normal. From these, 50 females and 50 males were selected randomly for the present study. Ages ranged from 29 to 79 for women (average = 45 ± 11 yr) and 27 to 68 for men (average = 45 ± 10 yr).

Tomographic Image Acquisition and Processing

Immediately after exercise, the patient was seated for a recovery period of 2–3 min and then walked to a SPECT imaging system (General Electric 400 ACT/STAR). The gamma camera was started in approximately the 45° right anterior oblique (RAO) view and rotated through an anterior 180° arc. Thirty-two planar views were obtained (40 sec/view). Data for each view were acquired into a 64 × 64 digital matrix with each picture element (pixel) in the array having a linear dimension of 6.2 mm. A 30-million count cobalt-57 (^{57}Co) flood acquisition was used to obtain uniformity correction factors for each pixel in the image. After the initial period of imaging, which required about 22 min, the patient was asked to return 3 hr after beginning the first image acquisition for delay images.

Before SPECT reconstruction, the images were analyzed for patient motion during acquisition by a program recently developed in this laboratory (*9*). This program was used to correct vertical motion of the subject if it exceeded 0.5 pixels (~ 3 mm). If there was horizontal motion, this was quantitated but could not be corrected. No subject in the present study had horizontal motion over 0.5 pixels.

Bull's-eye Processing and Quantitative Analysis

The signal to noise ratio in each of the acquired views was improved by convolving with a nine-point smoothing function. From the smoothed view data, one-pixel thick transaxial slices were reconstructed using a conventional ramp-filtered backprojection algorithm without any attenuation correction (General Electric 400 ACT/STAR). An oblique angle slice reconstruction procedure (General Electric 400 ACT/STAR) allowed reorientation of the transaxial planes so that slices corresponding to the three mutually perpendicular planes in a coordinate system fixed to the heart could be obtained (i.e., horizontal and vertical long axis and short axis).

Quantitative analysis (Digital Design Crystal V) was performed on each of the short axis slices. The procedure is shown in Figure 1. From apex to base, each short axis slice was subjected to a maximal count circumferential profile analysis similar to that performed in quantitative analyses of planar thallium view data (*10*). For all slices, except for the first two apical slices, the maximum count was determined along 40 radial vectors (i.e., nine-degree angular increments), which emanated from an operator-defined center of the left ventricle. For the first two slices, which generally do not have the doughnut-shaped appearance of the other short axis slices, the maximum count in the slice was obtained. After short axis slice selection and the placement of a cursor at the center of the left ventricle, the only other operator interaction involved in the analysis was the drawing of a circular region of interest about the left ventricular myocardial wall on the summed short axis slices. The circle established the boundary for the radial search procedure. The number of circumferential profile curves corresponded to the number of short axis slices. As shown in Figure 1, the extracted profile curve provides information on the distribution of ^{201}Tl in the walls of the myocardium. In our analysis program, as shown in Figures 1 and 2, the anterior wall, septal wall, inferior wall, and lateral wall are described by the radial vector segments 1–10 (0°–90°), 11–20

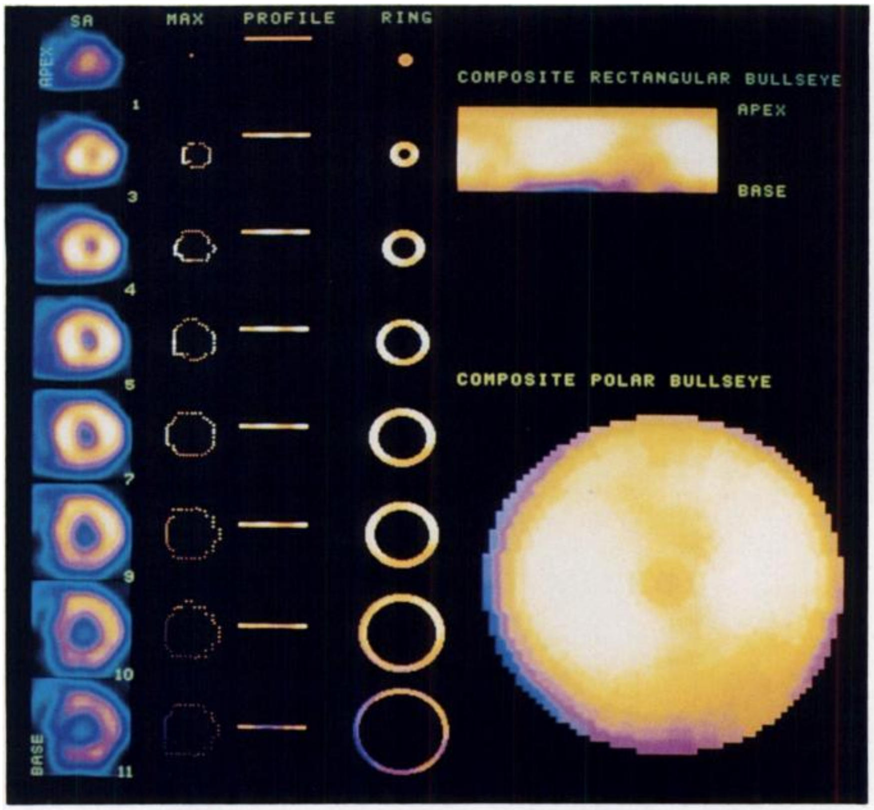

FIGURE 1
Schematic representation of the quantitative bull's-eye methodology. From an operator-defined left ventricular center, 40 radial vectors at nine-degree angular intervals are drawn; the maximum count along each of the radii is determined (second column). This is done on each of the short axis slices from apex to base. The circumferential profiles of maximum counts are arranged in a rectangular array (third column and upper right) with the vertical axis corresponding to slice number (apex to base) and the horizontal axis to angular position (anterior wall to septal wall to inferior wall to lateral wall). Maximum count is color coded with white being maximum and blue corresponding to ~ 40% of maximum. A polar coordinate transformation converts the rectangular array into the bull's-eye representation (fourth column and lower right). The source data for this figure are from a normal woman. Eight representative short axis slices from a total of 11 were selected for illustration.

(90°–180°), 21–30 (180°–270°) and 31–40 (270°–360°), respectively. In contrast to other approaches (*1*,*2*) no slice to slice normalization procedure was forced on the data so that relative count variations from slice to slice can be appreciated in the quantitative images. All the profiles were first displayed in a two-dimensional rectangular array (Fig. 1), where the horizontal axis corresponds to radial vector number (i.e., 1–40 or 0°–360°), and the vertical axis corresponds to slice number with the apex on top and the basal region on the bottom. The color in the image is associated with the count value in the profile curve. As shown in Figure 1, high count regions appear as white and low count regions appear as blue. A horizontal profile through a given portion of the rectangular array gives the maximal count profile curve appropriate to the short axis slice.

To simplify the analysis program we have fixed the patient rectangular array to consist of 15 slices. Patient data having more than 15 slices are automatically minified, and those with < 15 slices are magnified to conform to this convention. The magnification or minification is accomplished through an interpolation algorithm.

A more convenient display of the ^{201}Tl tomographic data is obtained by transforming the rectangular data array to polar coordinates, which effectively ties the 0° and 360° ends of the array together. This bull's-eye image, shown in Figures 1 and 2, has the counts corresponding to the apical region in the center while the counts in the basal region are shown in the outer portions.

The normal bull's-eye images reflect the average distribution of ^{201}Tl from the normal female and male populations. These images were obtained by averaging the counts from each of the 50 normal females and 50 normal males in each of the 600 (40 radial vectors multiplied by 15 slices) pixels in the rectangular array. The actual magnitude of ^{201}Tl uptake in each subject was not important to the present work, so each subject's array was scaled before averaging. This scaling was accomplished by multiplying the actual counts by the ratio of a subject-independent constant to the subject-dependent (total) counts in the midventricular region of the array (slices 4–12). This normalization is preferable to that which includes the apical and basal regions because these regions show more variability and depend more on the actual choice of slices as determined by the operator doing the analysis. As shown in Figure 2, each bull's-eye image was divided into 13 segments for quantitative analysis. Along with the normal (mean bull's-eye image, the standard deviation bull's-eye image was also calculated. The value of each pixel in this image reflects the variation of the normal subjects.

Analysis of Washout Data

We selected all patients for whom stress and delay image acquisitions were begun 170–190 min apart (180 ± 10 min) to minimize variability due to different delay times (37 females and 30 males). The absolute washout images were constructed using the actual counts in the stress and delay rectangular arrays. Relative washout used normalized arrays at stress and delay. In both cases, washout (%/100) = (stress − delay)/(stress).

Statistical Analysis

The mean and standard deviations of relative counts in each of the 13 regions were calculated. Comparisons were performed by Student's t-test for unpaired data, and differences were considered significant when $p < 0.05$. The male and female stress distributions were compared to those expected from a normal distribution.

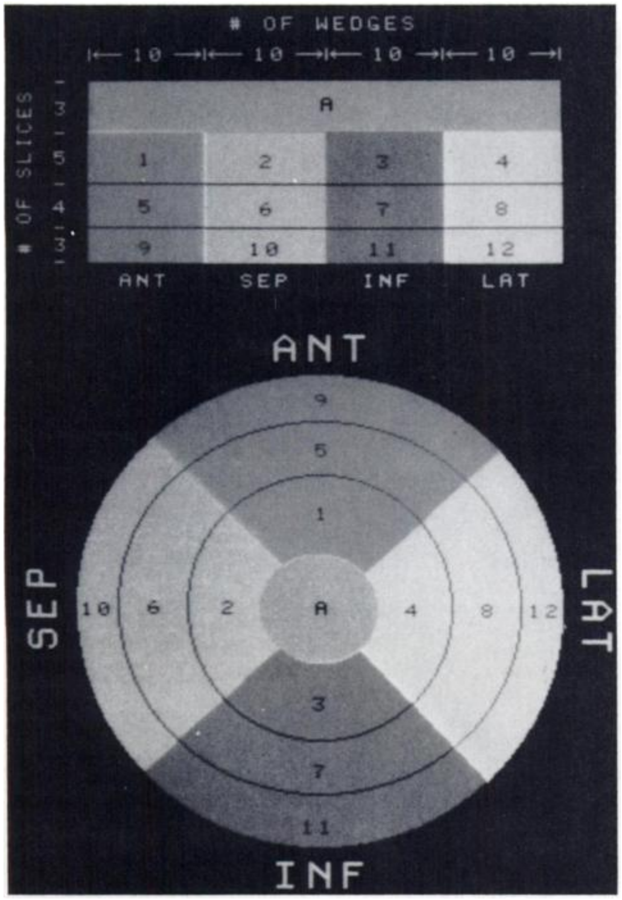

FIGURE 2
Bull's-eye segmentation for quantitative analysis.

RESULTS

Exercise Test Results

The results of the exercise tests are shown in Table 1 for the subjects whose data were included in washout analysis. Their exercise data were virtually identical to the larger groups of 50 females and 50 males. The exercise time on the Bruce protocol was greater in men than in women ($p < 0.01$), although the peak heart rates were nearly identical. Peak systolic blood pressures were not significantly higher in males than females.

TABLE 1
Exercise Test Data for Subjects Used in Washout Analysis Delay Time = 180 ± 10 (range) min

	Males	Females
n	30	37
Age (yr)	46 ± 12	45 ± 8
PHR (min^{-1})	171 ± 15	171 ± 16
PBP (mmHg)	175 ± 25	167 ± 23
EXT (min)	10.3 ± 3.1	8.1 ± 2.3*
WO (%)	40 ± 6	45 ± 8*

* $p < 0.01$ males vs. females.
PHR = Peak heart rate achieved.
PBP = Peak systolic blood pressure.
EXT = Exercise time, Bruce protocol.
WO = Washout for entire Bull's-eye (% decrease in counts in left ventricular myocardium from stress to delay).

Comparison Against Normal Distribution

Figure 3 shows the frequency distribution of the patient population (solid curve) of the average counts in the anterior, septal, inferior, and lateral walls in the midventricular region of the stress bull's-eye image for males and females. The mean and standard deviation ($\bar{x} \pm$ s.d.) determined from these curves was used to generate the normal distributions ("x" – points) in Figure 3, which correspond well with the patient curves.

Comparison of Male and Female Bull's-eye Images

Figure 4 shows the male and female bull's-eye images at stress and delay. The corresponding 13 segment

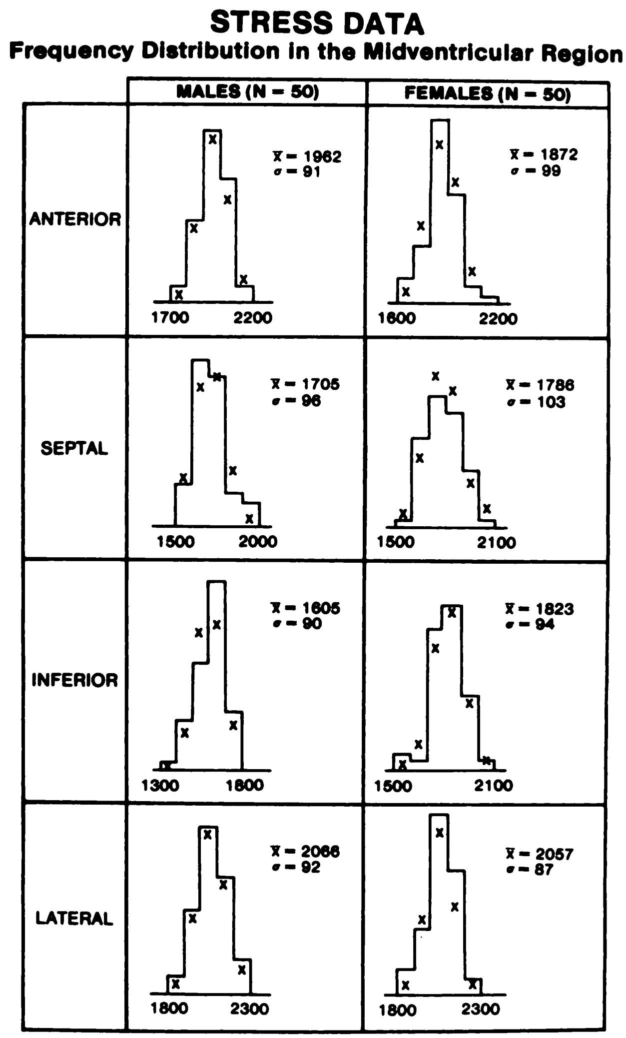

FIGURE 3
The frequency distribution (solid curve) of the patient population for each of four regions from the stress bull's-eye image for males (left) and females (right). The x-points are derived from a normal distribution with $\bar{x}$ and sigma as shown.

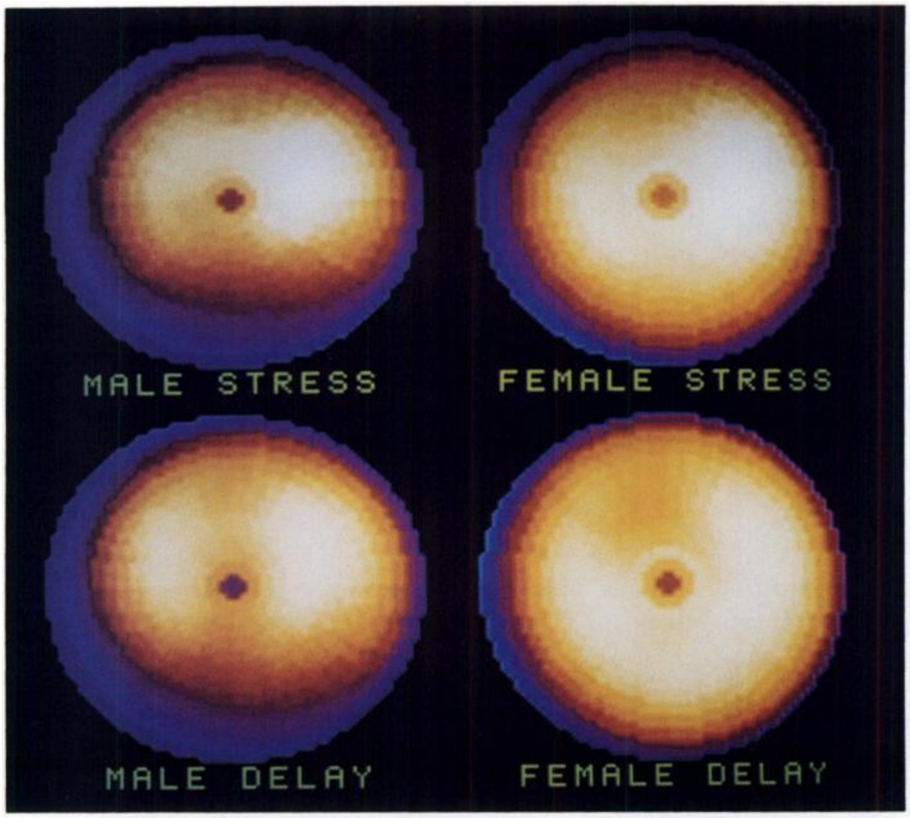

FIGURE 4
Differences in appearance of color-coded bull's-eye images on stress (above) and delay (below) in males (left) and females (right). Note that the lateral wall is brightest, and there are mild decreases in counts in the anterior wall in females, and large decreases in the inferior wall in males on stress and delay. These bull's-eyes are derived from 50 male and 50 female subjects.

numerical displays in Figures 5 and 6 show the relative ratios with respect to the region with the highest counts (region 4 in the lateral wall) at stress and delay, respectively. The bull's-eye images show significant differences between males and females at stress and delay (stress: 9/13 regions, $p < 0.05$; delay: 10/13 regions, $p < 0.05$). The relative percent differences between males and females at stress and delay are shown in Figure 7.

For males at stress and delay:

1. Each septal wall segment from apex to base showed decreased counts compared to the corresponding lateral wall segment.
2. Each inferior wall segment from apex to base showed decreased counts compared to the corresponding anterior wall segment.
3. The apical region showed decreased counts compared to adjacent septal, anterior, and lateral wall segments, but approximately the same counts as the adjacent inferior wall segment.

For females at stress and delay:

1. As for males, each septal wall segment from apex to base showed decreased counts compared to the corresponding lateral wall segment.
2. In contrast to males, each inferior wall segment

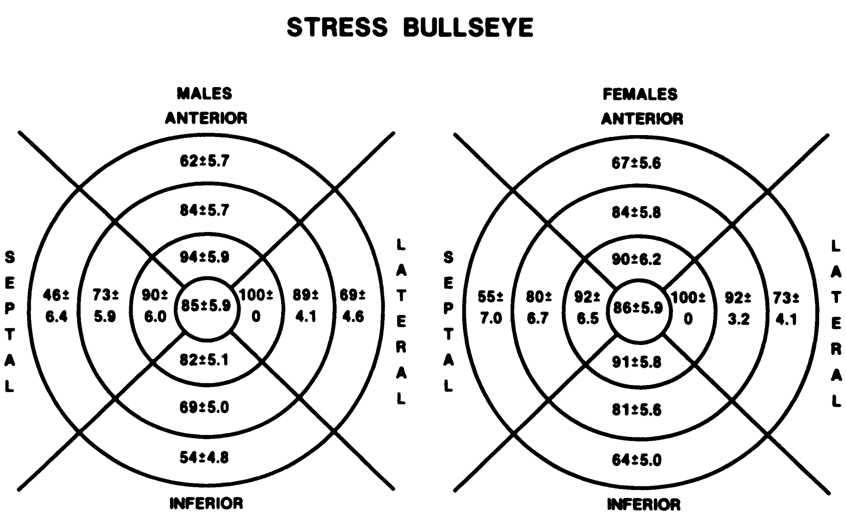

FIGURE 5
Bull's-eyes are shown at stress for males (left) and females (right). Each region is expressed as a percentage ($\bar{x} \pm$ sd) of the counts in the lateral wall region that has the highest counts.

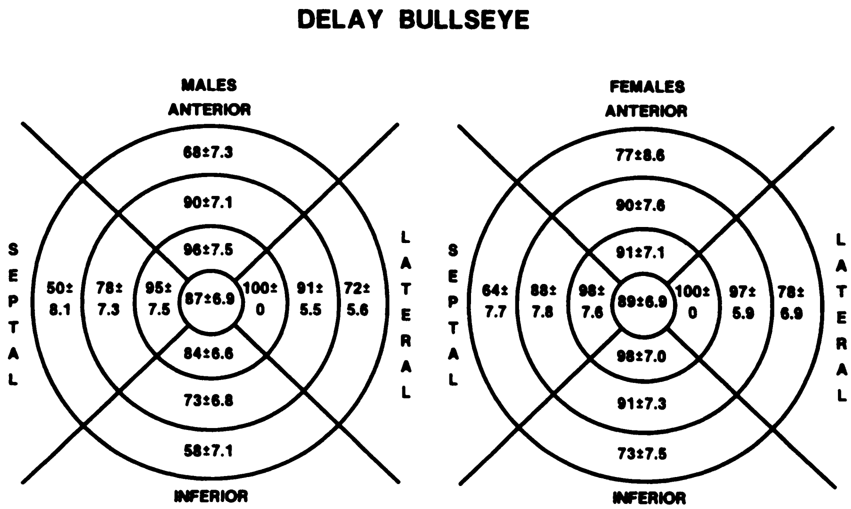

FIGURE 6
Bull's-eyes are shown at delay for males (left) and females (right). Each region is expressed as a percentage ($\bar{x} \pm$ sd) of the counts in the lateral wall region that has the highest counts.

from apex to base showed similar counts compared to the corresponding anterior wall segment.

3. As for males, the apical region showed decreased counts compared to adjacent septal, anterior, and lateral wall segments; however, in contrast to males the apical region also showed decreased counts compared to the adjacent inferior wall segment.
4. In general, the female bull's-eye image shows less segmental variation than the male bull's-eye image.

Thallium-201 Washout Differences

Comparisons of stress versus delay bull's-eye images showed significant differences for both males (9/13 regions, $p < 0.05$) and females (10/13 regions, $p < 0.05$). Larger percent changes are seen in the female distributions (see Fig. 8 for relative washout).

The absolute values of washout (Fig. 9) showed slower washout in males than in females for all regions of the bull's-eye ($p < 0.05$ for 10/13 regions). For the whole bull's-eye, the washout rate was $(40 \pm 6)\%$ in males and $(45 \pm 8)\%$ in females ($p < 0.01$, males versus females). In Figure 10 and Figure 11, the washout bull's-eyes for each gender are shown for those subjects with ages less than or greater than 45 yr old, respectively. The differences between the genders in washout rate occur mainly in the younger group (11/13 regions with $p < 0.05$ in the younger group versus 1/13 regions with $p < 0.05$ in the older group). We find no strong relationship between the washout rates and peak exercise heart rate, percent age-predicted maximum heart rate, body surface area, or peak systolic blood pressure.

DISCUSSION

The results of the present study are important because they define the expected range of normals in SPECT ^{201}Tl stress, delay, and washout distributions with a larger database than previously reported. This information is crucial to quantify differences in ^{201}Tl distributions for the diagnosis of CAD. Differences in body habitus and resulting attenuation, as well as differences in size, shape, and position of the heart may all alter the relative count density in the reconstructed SPECT

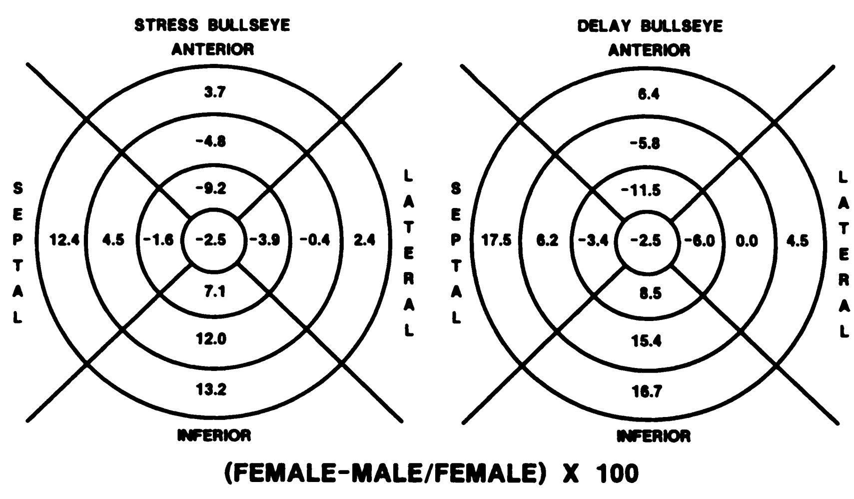

FIGURE 7
The 13 segment display showing relative differences between males and females at stress and delay.

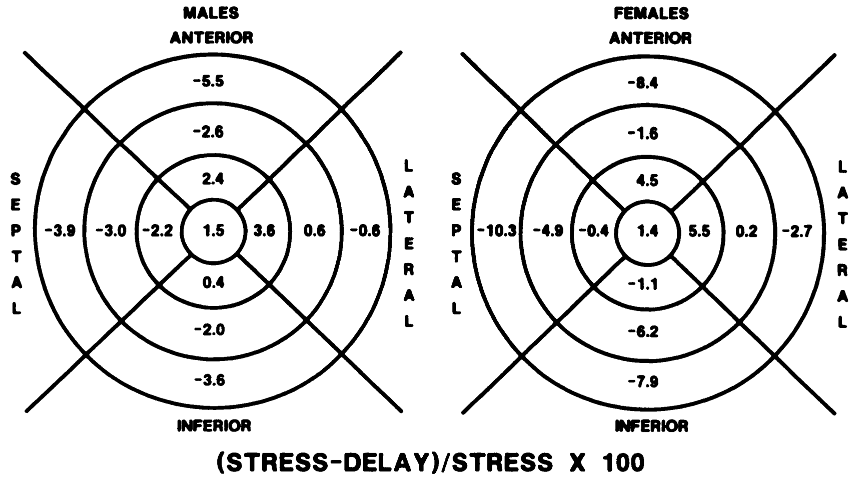

FIGURE 8
The 13 segment display showing relative differences between stress and delay for males and females.

images independent of myocardial perfusion (*11*). Since programs which can correct for variable attenuation are not currently available, the best way to deal with this variability is to define a normal file and to compare any one individual with this file quantitatively. The variability in ^{201}Tl uptake is normally distributed among individuals with a low probability of CAD in the present study (Fig. 3). This observation validates the use of parametric statistics such as the mean and standard deviation to describe the variability. Thus, the likelihood of CAD in any one individual can be estimated by determining the number of standard deviations that an area on his or her bull's-eye falls below the mean of the normal file (*12,13*).

The major findings of the study emphasize differences between females and males in the stress, delay, and washout distributions of SPECT ^{201}Tl myocardial perfusion scans. The females showed 4.8%–9.2% fewer counts in the anterior wall at stress than did the males. On the other hand, the males showed 7.1%–13.2% fewer counts in the inferior wall than did the females. Other features of the images in females and males deserve mention. The region with the most ^{201}Tl activity is the lateral wall near the apex. In general, beyond the center of the bull's-eye (the apex), the apical midventricular regions had more ^{201}Tl activity than did the more basal regions. From a physiologic standpoint, we would expect a more homogeneous distribution of ^{201}Tl in the myocardium than is observed in the SPECT images. There is evidence from animal studies to indicate that there are only minor systematic differences in blood flow to different regions of the left ventricle as measured by radiolabeled plastic microspheres during treadmill exercise or rest (*14,15*). Presumably, the relative decrease in ^{201}Tl activity in the anterior wall in females is due to breast tissue attenuation (*12*); the relative decrease in ^{201}Tl activity in the inferior wall in males may be due to diaphragmatic attenuation. In our limited experience with ^{201}Tl images in females after mastectomies, the pattern resembles the male normal file. Further, in a small number of males with gynecomastia, we have observed mild decreases in ^{201}Tl counts in the anterior wall. The location of maximum counts in the lateral wall has been predicted by previous work from this laboratory using a simulated cardiac model with variable attenuation and resolution (*11*). The greater

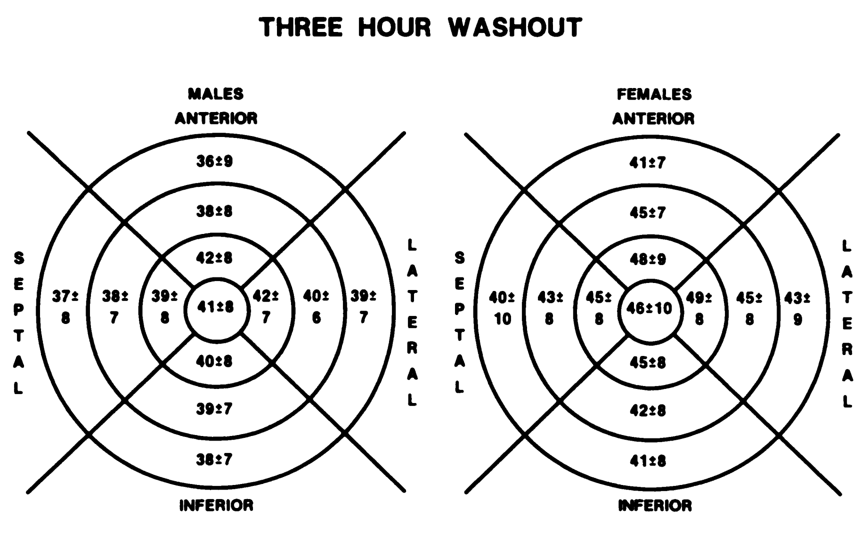

FIGURE 9
The 13 segment absolute washout display showing significant differences between males and females.

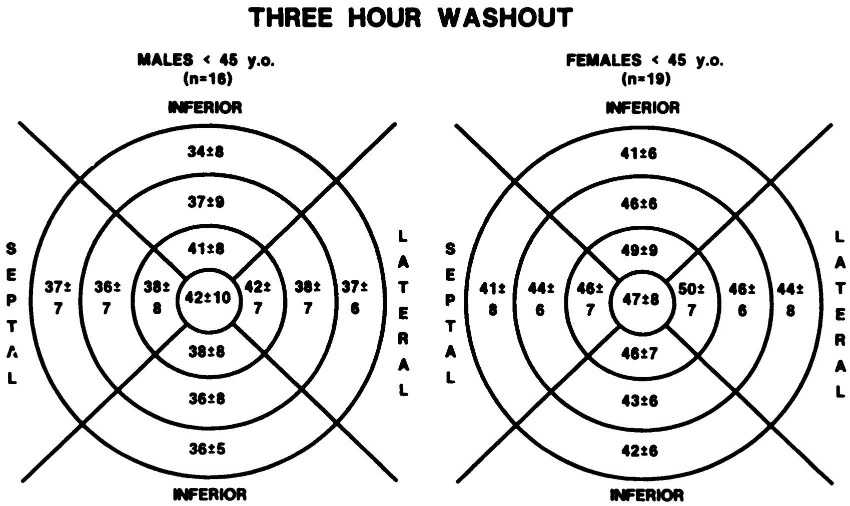

FIGURE 10
The 13 segment absolute washout display showing significant differences between males and females < 45 yr old.

^{201}Tl activity in the apical-midventricular region than in the basal region may be related to the thinning of the base of the left ventricle as it nears the mitral valve plane (*15*) or to the effects of variable attenuation and resolution (*11*). The papillary muscles may also contribute to midventricular ^{201}Tl activity.

The faster washout in women versus men was significant only for persons < 45 yr of age, not for persons > 45 yr of age. The faster washout in females cannot be explained with certainty but is not likely to be due to differences in attenuation between females and males, since attenuation due to chest wall anatomy should remain constant between stress and delay images. Also, faster washout in women occurs in the inferior, inferoseptal, and inferolateral segments which should not be influenced by breast tissue attenuation. It is possible that the females had higher peak coronary blood flow during exercise than did the males, even though their peak heart rates and blood pressures were similar. However, they had reduced exercise times on the treadmill. In upright bicycle exercise, females show less increase in ejection fraction but a greater increase in left ventricular end-diastolic volume, compared to males (*16*). These changes might increase myocardial oxygen demand and coronary blood flow and ^{201}Tl washout rate in females more than in males because the increased ventricular volume would increase preload and afterload. On the other hand, the higher left ventricular ejection fraction in males would suggest that myocardial contractility would be increased more in men than in women, which should increase myocardial oxygen demand and coronary blood flow (*17*) and ^{201}Tl washout rate more in males than in females. This issue cannot really be resolved without direct measurements of coronary blood flow. The higher washout rate in females may also be related to differences in body composition of females and males, which could cause different distributions of ^{201}Tl during stress and delay conditions. It should be noted, however, that washout rate did not correlate with body surface area in women. The washout rate difference between females and males has also been noted on planar exercise ^{201}Tl imaging

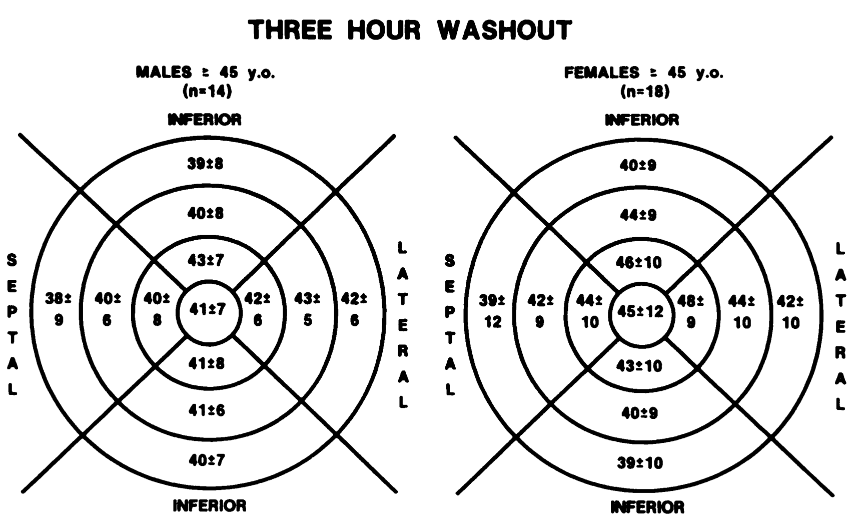

FIGURE 11
The 13 segment absolute washout displays for subjects at least 45 yr old.

(*18*). Whatever the cause, it is obviously important to account for this difference in diagnostic applications of exercise ^{201}Tl.

Critique of Methods

Our subjects were classified as normal by their clinical and exercise ECG data. All subjects had been referred by their personal physicians for exercise ^{201}Tl imaging to rule out coronary disease, so that none were healthy volunteers. All were defined as normal without knowledge of the ^{201}Tl image data, and none had cardiac catheterization. Defining normal subjects without cardiac catheterization avoided potential selection basis (*19*) since subjects are often referred for cardiac catheterization based on positive noninvasive test results or histories of more severe chest pain (*5,19*). Despite having < 50% coronary arterial narrowing on angiograms, many of these ("cath normal") patients may have some other form of heart disease. The most obvious potential error due to our method of selecting a normal file would be to include a few subjects with some large vessel coronary disease, but this should affect < 5% of our subjects, based on our selection criteria.

In conclusion, these results define quantitatively the normal range of the SPECT ^{201}Tl myocardial images. There are important differences between females and males, which require the use of separate normal reference files for quantitative analysis.

REFERENCES

1. Caldwell JH, Williams DL, Harp GL, et al. Quantitation of size of relative myocardial perfusion defect by single photon emission computed tomography. *Circulation* 1984; 70:1048–1056.
2. Garcia EV, Van Train K, Maddahi J, et al. Quantification of rotational thallium-201 myocardial tomography. *J Nucl Med* 1985; 26:17–26.
3. Johnson TK, Kirch DL, Hasegawa BH, et al. A concentric polar plotting for analysis of emission cardiac tomography [Abstract]. *J Nucl Med* 1981; 22:P40.
4. Eisner RL, Churchwell A, Noever T, et al. Quantitative analysis of the tomographic thallium-201 myocardial bullseye display: critical role of correcting for patient motion. *J Nucl Med* 1988; 29:91–97.
5. Patterson RE, Horowitz SF, Eng C, et al. Can exercise electrocardiography and thallium-201 myocardial imaging exclude the diagnosis of coronary artery disease? *Am J Cardiol* 1982; 49:1127–1135.
6. Patterson RE, Eng C, Horowitz SF. Practical diagnosis of coronary artery disease: a Baye's theorem nomogram to correlate clinical data with noninvasive tests. *Am J Cardiol* 1984; 53:252–256.
7. Kannel WB, Gordon T. The Framingham study: an epidemiologic investigation of cardiovascular disease, Vol 12. Bethesda: National Heart, Lung, and Blood Institute; 1968.
8. Diamond GA, Forrester JS. Analysis of probability as an aid in the clinical diagnosis of coronary artery disease. *N Engl J Med* 1979; 300:1350–1358.
9. Eisner RL, Noever T, Nowak DJ, et al. Use of cross-correlation to detect patient motion during SPECT imaging. *J Nucl Med* 1987; 28:98–101.
10. Watson DD, Campbell NP, Read EK, et al. Spatial and temporal quantitation of planar thallium myocardial images. *J Nucl Med* 1981; 22:577–584.
11. Eisner RL, Nowak DJ, Pettigrew RI, Fajman W. Fundamentals of 180 degree acquisition and reconstruction in SPECT imaging. *J Nucl Med* 1986; 27:1717–1728.
12. Cloninger KG, Eisner RL, Oates J, et al. Specificity of SPECT Tl-201 myocardial imaging in women: improvement by adjusting for breast tissue attenuation [Abstract]. *J Am Coll Cardiol* 1987; 9:140A.
13. Shonkoff D, Eisner RL, Gober A, et al. What quantitative criteria should be used to read defects on the SPECT Tl-201 bullseye display in men? ROC analysis [Abstract]. *J Nucl Med* 1987; 28:P674–675.
14. Ball RM, Bache RJ, Cobb FR, Greenfield JCJ. Regional myocardial blood flow during graded treadmill exercise in the dog. *J Clin Invest* 1975; 55:43–51.
15. Schlant RC, Silverman ME. Anatomy of the heart. In: Hurst JW, Logue RB, Rackley RB, et al, eds. *The heart*, 6th ed. New York: McGraw-Hill Book Co.; 1986: 16–36.
16. Higginbotham MB, Morris KG, Coleman RE, Cobb FR. Sex-related differences in the normal cardiac response to upright exercise. *Circulation* 1984; 70:354–366.
17. Gregg DE, Fischer LC. Blood supply to the heart. In: Hamilton WF, ed. *Handbook of physiology, circulation.* Washington, DC: American Physical Soc.; 1963: 1517–1584.
18. Rabinovitch M, Suissa S, Elstein J, et al. Sex-specific criteria for interpretation of thallium-201 myocardial uptake and washout studies. *J Nucl Med* 1986; 27:1837–1841.
19. Rozanski A, Diamond GA, Forrester JS, Swann HJC. Alternative reference standards for cardiac normality: implications for diagnostic testing. *Ann Int Med* 1984; 101:164–166.